

Spatial Sampling Design for Estimating Regional GPP With Spatial Heterogeneities

Jianghao Wang, Yong Ge, Gerard B. M. Heuvelink, and Chenghu Zhou

Abstract—The estimation of regional gross primary production (GPP) is a crucial issue in carbon cycle studies. One commonly used way to estimate the characteristics of GPP is to infer the total amount of GPP by collecting field samples. In this process, the spatial sampling design will affect the error variance of GPP estimation. This letter uses geostatistical model-based sampling to optimize the sampling locations in a spatial heterogeneous area. The approach is illustrated with a real-world application of designing a sampling strategy for estimating the regional GPP in the Babao river basin, China. By considering the heterogeneities in the spatial distribution of the GPP, the sampling locations were optimized by minimizing the spatially averaged interpolation error variance. To accelerate the optimization process, a spatial simulated annealing search algorithm was employed. Compared with a sampling design without considering stratification and anisotropies, the proposed sampling method reduced the error variance of regional GPP estimation.

Index Terms—Anisotropy, block kriging, spatial simulated annealing, stratification.

I. INTRODUCTION

THE total amount of gross primary production (GPP) in an ecological system plays an important role in the evaluation of regional vegetation primary production and storage of carbon as biomass [1], [2]. Accurate estimation of GPP is essential for monitoring the global or regional carbon cycle [3], [4]. In practice, there are two groups of ways for estimating GPP [5]: one group makes use of remote sensing data while another makes estimates based on ground samples [6]. As an example of the first group of methods, GPP estimates are now being based on the observations from the Moderate Resolution Imaging Spectroradiometer (MODIS) sensor. However, validation studies showed that remote sensing-based GPP estimates may not always be accurate and may be biased [2]. Compared with remote sensing methods, ground sampling uses much fewer observations but the individual observations are more accurate. With a proper sampling design and statistical prediction model, ground sampling can achieve levels of accuracy that are suffi-

Manuscript received September 29, 2012; revised April 10, 2013 and June 25, 2013; accepted July 9, 2013. Date of publication September 5, 2013; date of current version November 25, 2013. This work was supported in part by 863 High Technology of China (2012AA12A305) and the National Natural Science Foundation of China under Grant 40971222. (Corresponding author: Y. Ge.).

J. Wang, Y. Ge, and C. Zhou are with the State Key Laboratory of Resources and Environmental Information System, Institute of Geographic Sciences and Natural Resources Research, Chinese Academy of Sciences, Beijing 100101, China (e-mail: ge@lreis.ac.cn).

G. B. M. Heuvelink is with the Chairgroup Soil Geography and Landscape, Wageningen University, 6708 PB Wageningen, The Netherlands.

Digital Object Identifier 10.1109/LGRS.2013.2274453

cient for most intended purposes [7]. Hence, sampling has been widely used in the estimation of regional GPP [8].

The main factors that influence the error variance of GPP sampling estimation are the sample size, the sampling design, the measurement error of the observations, and uncertainties in the (geo)statistical model used to represent the spatial distribution of GPP. Much attention has been paid on the geostatistical modelling and associated estimation methods in the environmental sciences, such as the development of various types of kriging algorithms [9]. However, the choice of sample size and sampling design are often overlooked in real-world applications, also for regional GPP estimation [2], [8]. Simple random sampling, systematic sampling and stratified random sampling are common sampling methods that are often employed in a design-based context [10], [11]. Model-based inference is an alternative approach that may be applied to spatial sampling problems and used to exploit the spatial structure in the data [12]. Since in most practical cases GPP is spatially autocorrelated, we use a model-based approach to optimize the sampling locations. Geostatistical sampling design optimization typically aims at minimizing the average kriging prediction error variance. It has been widely used in environmental sampling design optimization [13]–[17]. Nevertheless, for the purpose of estimating the regional mean or total amount of GPP, the goal changes into the minimisation of the global estimation error variance. In this context, the support of the estimate changes from spatial points to a block (i.e., the region of interest) and the sampling design is optimized by minimizing the block kriging error variance [18], [19]. Note that the block to be estimated need not be rectangular but can be irregular and indeed may take the shape of the region of interest.

Previous research on geostatistical sampling and modelling for estimation of GPP is based on the assumptions of stationary and isotropy of GPP over the study area. In practice, it is hard to meet these assumptions because the surface mean and variance of GPP may change considerably across space [20], [21]. Besides, spatial correlation may depend on direction (i.e., anisotropy), which is also a form of heterogeneity that may be present in GPP and will influence the optimal sampling design [19]. Therefore, there is a need to develop sampling strategies for GPP estimation in case of spatial heterogeneity exhibited by nonstationarity and anisotropy of GPP. In this letter, we present a method to optimize the spatial sampling design in a spatial heterogeneous area by combining stratified block kriging [22] with an anisotropic spatial covariance structure. This methodology uses spatial simulated annealing and is illustrated with a real-world application. The objective is to design a sampling protocol for estimating the regional total amount of GPP in the Babao river basin, China.

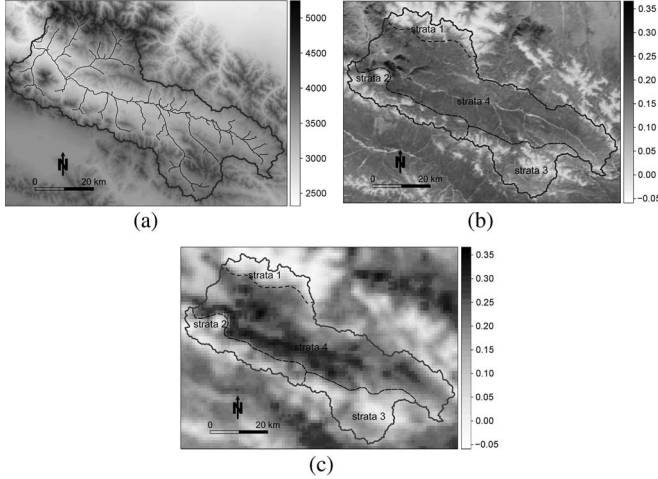


Fig. 1. Babao river basin. (a) Digital elevation model and river distribution; (b) annual mean NDVI retrieved from MODIS; and (c) annual mean GPP estimated from MODIS. The area is stratified into four strata.

II. MATERIALS AND METHODS

A. Study Area and Data Description

The area of interest is the Babao river basin located in the upstream part of the Heihe river basin, China. The Babao river basin is located between $37^{\circ} 43' N - 38^{\circ} 20' N$ and $100^{\circ} 05' E - 101^{\circ} 09' E$ and covers an area of 2503 km^2 [Fig. 1(a)]. Elevation ranges from 2339 m to 4947 m and annual average temperature is between -7°C and 3°C . Vegetation in the Babao basin is mainly grassland and mountain forest. Along the river with lower elevations, there are rangelands including mountain meadows, bushy vegetation, middle mountain forests and meadows. Above 4500 m there is a glacier and snow-covered zone. Owing to differences in weather, topography, soil condition and land cover type, the landscapes in the Babao river basin depict important spatial heterogeneities.

To acquire the vegetation distribution in the Babao river basin, MODIS remote sensing estimates of GPP (MOD 17A3, with a spatial resolution of 1 km) and the normalized difference vegetation index (NDVI, MOD 13Q1, with a spatial resolution of 250 m) were downloaded from the NASA Level 1 and Atmosphere Archive and Distribution System (LAADS FTP). The topography and directional effects on the MODIS GPP and NDVI were first corrected [23]. Then the images were mosaicked and reprojected to the UTM projection system (zone 47) with a nearest neighbor resampling method. Next the annual mean NDVI and GPP were obtained by calculating the mean value over all images collected throughout the year 2012. The results are shown in Figs. 1(b), (c).

B. Sampling Optimization of GPP With Spatial Heterogeneities

To address the nonstationarity in the GPP in the Babao river basin, the study area was decomposed into smaller subareas (strata) that are more homogeneous. Under the assumption of stationarity within strata, stratified block kriging (StrBK) is appropriate to provide the best linear unbiased estimator (BLUE) of the total amount of GPP [22].

Stratified Block Kriging: StrBK applies separate block kriging (BK) to the different strata. For the i th stratum v_i over the study area \mathcal{A} , StrBK proceeds in three steps.

- 1) Stratification. Considering the spatial distribution of GPP, \mathcal{A} is first divided into p strata. Each stratum is regarded as a block. The i th stratum \mathcal{A}_i is defined as the set of locations \mathbf{u} belonging to the stratum v_i . In practice, strata may be formed on the basis of prior knowledge, an effective proxy variable, and the distribution of other variables that are known to affect target distribution [24]. Here the stratification was based on an unsupervised classification of the MODIS GPP imagery (see Section III).
- 2) Anisotropic covariance or variogram calculation. The covariance of GPP, $\hat{C}(\mathbf{h}; v_i)$ (where \mathbf{h} is the spatial lag) is calculated and a covariance function or variogram is fitted within each stratum. Since field samples data were lacking, the MODIS GPP data were adopted for variogram calculation. In this step, it is important to account for directional effect in the covariance structure, when it is present. The simplest way to model the directional effect on the covariance structure is called *geometric anisotropy* [25]. This arises when the covariance function can be transformed to an isotropic covariance by rotating and stretching the coordinate axes. Algebraically, a model with geometrical anisotropy in spatial lag $\mathbf{h} = (h_x, h_y)$ can be converted to a stationary model in lag $\mathbf{h}' = (h'_x, h'_y)$ by

$$\mathbf{h}' = \mathbf{h} \begin{bmatrix} \cos(\theta) & -\sin(\theta) \\ \sin(\theta) & \cos(\theta) \end{bmatrix} \begin{bmatrix} 1 & 0 \\ 0 & \varphi^{-1} \end{bmatrix} \quad (1)$$

where θ is the *anisotropy angle* and φ is the *anisotropy ratio*, which are estimated by a nonparametric identification method [26]. The direction along which the correlation decays most slowly with increasing distance is called the *principle axis*.

- 3) Total GPP and its error variance estimation. The mean value of GPP in each stratum $\hat{z}(v_i)$ is estimated using BK with an anisotropic variogram model and all observations within the stratum. The corresponding block kriging prediction error variance $\sigma_{BK}^2(v_i)$ in each stratum is given by [18]

$$\sigma_{BK}^2(v_i) = \mathbf{c}_{v_i, v_i} - \mathbf{c}'_{v_i} \mathbf{C}^{-1} \mathbf{c}_{v_i} + \mathbf{d}' (\mathbf{I} \mathbf{C}^{-1} \mathbf{I})^{-1} \mathbf{d} \quad (2)$$

where $\mathbf{d} = 1 - \mathbf{I}' \mathbf{C}^{-1} \mathbf{c}_{v_i}$, \mathbf{I}' is an n -dimensional row-vector whose elements are set to unity, \mathbf{c}_{v_i, v_i} is the block-to-block covariance, \mathbf{c}_{v_i} is the vector of covariances between the GPP at the sampling points and the prediction block (point-to-block covariances), \mathbf{C} is the variance-covariance matrix of the GPP at the sampling points (point-to-point covariances). \mathbf{c}_v and \mathbf{C} are derived from the variogram.

Based on the assumption that there is no between-stratum correlation, the total GPP is estimated as $\hat{z}_{StrBK} = \sum_{i=1}^p A_i \cdot \hat{z}(v_i)$, and the corresponding prediction error variance of the total GPP is $\sigma_{StrBK}^2 = \sum_{i=1}^p A_i^2 \cdot \sigma_{BK}^2(v_i)$. Here, A_i is the area of stratum i . Note that calculation of σ_{BK}^2 and σ_{StrBK}^2 only requires the variogram derived from proxy MODIS GPP, and not the GPP field observations themselves. This attractive property allows one to estimate the error variance prior to

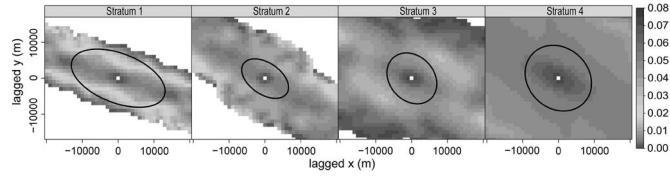


Fig. 2. MODIS GPP variogram maps for the four strata. The black line is the fitted geometric anisotropy ellipse.

collecting data, and it is this property that will be used in the GPP sampling optimization below.

Sample Design Optimization With Spatial Simulated Annealing: Given the StrBK model, the objective is to optimize the GPP sampling locations such that the smallest value for the σ_{StrBK}^2 is obtained. We denote this variance by AStrBKV. Thus, after determining the sample size, the next task is to determine the optimum sampling locations. To accelerate this optimization process, spatial simulated annealing (SSA) was employed.

SSA is the spatial extension of simulated annealing, for solving spatial optimization problems [14]. SSA uses the idea of simulated annealing to search for the minimum of a given objective function (i.e., the AStrBKV), for which an exhaustive search is practically impossible. Starting from an arbitrary initial sampling design, the optimization progresses iteratively by moving a randomly chosen sampling location over some distance, each time calculating the objective function and always accepting improved sampling designs. To avoid the objective function being trapped in a local minimum, deteriorating designs are accepted with some probability (generally set to $\chi \geq 0.2$). This probability is gradually decreased as the iteration continues. In this letter, we adopted the most commonly used cooling schedule, whereby χ was initially set to 0.2 and gradually decreased as the iteration progressed to ensure convergence [14], [16]. The SSA procedure was stopped when there was no improvement in the criterion over 200 iterations. All analyses and optimizations were implemented using a set of functions written in the R language.

III. RESULTS

The spatial sampling design in the Babao river basin was optimized based on the StrBK model-based optimization algorithm described above. First, according to the spatial distribution of MODIS GPP shown in Fig. 1(c), the *k-means* algorithm [24] was adopted to perform an unsupervised spatial clustering of GPP. In this process, the *k-means* method led to seven classes with isolated small areas that were merged to maintain spatial continuity in each stratum, resulting in four areas, as shown in Fig. 1(c). The MODIS land cover map was not used since its associated quality flags provide a large misclassification rate, with a low overall accuracy (60%). The stratification also matched that of the higher resolution MODIS NDVI map in Fig. 1(b), which is strongly correlated with the GPP ($R^2 = 0.89$).

To model the spatial variability of the GPP for each stratum, the *variogram map* and *anisotropy variogram* were calculated and appropriate variogram models were fitted. First, a variogram map for each stratum was calculated to assess the degree of anisotropy and major direction of spatial continuity (Fig. 2). As seen in Fig. 2, the GPP appears to be spatially autocorrelated for a long distance along the NW-SE direction, hence NW-

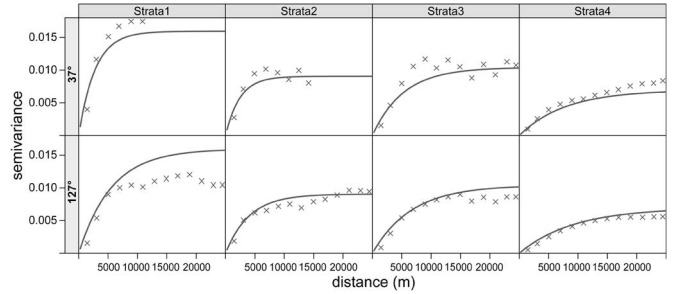


Fig. 3. GPP experimental variograms in two main directions for the four strata (crosses) and the fitted with exponential models (solid lines). Here, 127° and 37° are the principal axis angle and the minor axis angle, respectively.

TABLE I
PARAMETERS OF THE EXPONENTIAL VARIOGRAM MODELS

Stratum	Principle axis			Anisotropy angle (°)	Anisotropy ratio
	Nugget	Sill	Range (m)		
stratum 1	0.001	0.016	16130	121	2.00
stratum 2	0.001	0.009	8637	123	1.67
stratum 3	0	0.010	9091	131	1.25
stratum 4	0	0.007	9234	133	1.18
strata mean ^a	0	0.010	10773	127	1.53
whole region	0	0.019	11662	—	—

^astrata mean is the average value of parameters in strata 1 - 4.

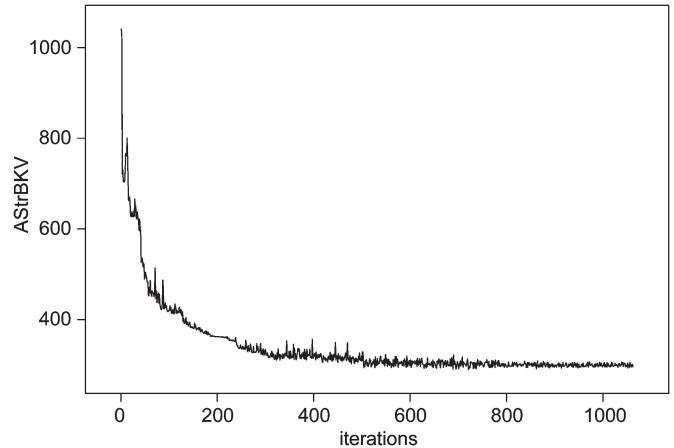


Fig. 4. Convergence of objective function with increasing SSA iterations (shown for the case where the sample size is 50).

SE should be considered as the principle axis. Following this, geometric anisotropy was modeled by defining a range *ellipse*. Taking the principal axis angle as 127° and minor axis angle as 37° (measured in positive degrees, clockwise from the Y-axis), the anisotropic variogram was calculated and fitted with an exponential model, as shown in Fig. 3. The fitted parameters are presented in Table I. The fitted variograms show that the GPP is spatially autocorrelated in every stratum, and has a significant anisotropy variogram structure. Stratum 1 has the largest range, sill and anisotropy ratio, whereas stratum 4 is more homogeneous, with the smallest sill and anisotropy ratio. Besides, an isotropic variogram for the whole region was calculated and fitted with an exponential model, as listed in Table I.

To determine a proper GPP sample size, the relationship between the sample size and the corresponding minimum objective function value was investigated. Fig. 4 shows the convergence of the AStrBKV as the SSA progressed for the case where the sample size is 50. The minimum objective function

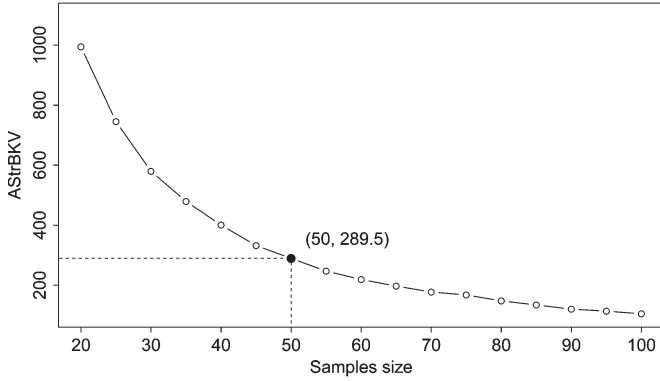


Fig. 5. Trade-off between objective function AStrBKV and sample size.

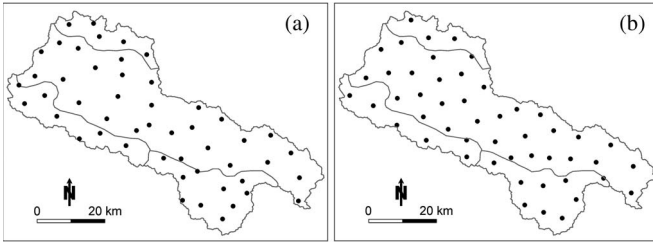


Fig. 6. Optimized 50 GPP sampling design in the Babao river basin. (a) StrBK model-based sampling with anisotropic variogram model; (b) ordinary BK model with isotropic variogram model.

TABLE II
SUMMARY OF SAMPLES STATISTICS

Method	Region	Area (km ²)	$A^2 \cdot \sigma_{BK}^2$	Sample size	Sampling density
StrBK sampling	stratum 1	193	43.3	5	0.026
	stratum 2	312	48.2	7	0.022
	stratum 3	405	63.8	10	0.025
	stratum 4	1589	134.2	28	0.018
Ordinary BK sampling	whole region	2499	321.9	50	0.020

value for various sample sizes is shown in Fig. 5. It can be seen that the AStrBKV value decreases with increasing sample size. When the sample size reached 50, the increase of samples did not substantially reduce the error variance of regional GPP estimation. Therefore, based on a trade-off between sampling costs, accuracy requirement, and budget constraints, the total sample size was set to 50. In addition, the SSA algorithm allocated these to the strata and achieved the optimized sample size for each stratum.

Finally, taking AStrBKV as the objective function, 50 GPP sample locations were obtained with SSA. As expected, the prediction error variance improved with the increase of SSA iterations (Fig. 4). After 1062 iterations, AStrBKV obtained a value of $\sigma_{StrBK}^2 = 289.5$. Then, the optimized samples location was obtained, as shown in Fig. 6(a). The 50 samples are fairly uniformly distributed over the study area, although there are some interesting deviations from a completely uniform distribution. In each stratum, the distance between samples in the direction of the principle axis of the anisotropic variogram is larger than in the direction of the minor axis because spatial correlation is stronger in the direction of the principle axis. Summary statistics are listed in Table II. It shows that stratum 1 has the smallest area and has a relatively high sampling density, while stratum 4 has the largest area and the lowest sampling

density. The differences in sampling density are caused by the degree of spatial variability within each stratum. Table I shows that stratum 1 has the largest variability (sill = 0.016) while stratum 4 has the smallest (sill = 0.007).

For comparison, a sampling design with no stratification and isotropic variogram model for the whole region was optimized by using an ordinary BK model-based sampling method [19]. The result is shown in Fig. 6(b). As expected, the sampling locations are uniformly distributed. With the same StrBK model and anisotropic variogram, the estimation error variance of this design is $\sigma_{StrBK}^2 = 321.9$ (Table II), which is larger than the design in Fig. 6(a). This comparison indicates that regional GPP estimation error variance may decrease with 10.1% by considering stratification and anisotropy in modelling the spatial variability of GPP.

IV. DISCUSSION

During GPP sampling optimization, it is important to identify the type of heterogeneity characterizing the spatial distribution of GPP. Wang *et al.* [21] indicated two kinds of heterogeneities: one type refers to an attribute with a spatial variable mean (nonhomogeneity in the mean), and another one refers to an attribute with a variance that changes over space (nonhomogeneity in the variance). Besides that, directional structure can be considered as another kind of heterogeneity [22]. In practice, nonhomogeneity in the means may be characterised by a spatial trend or a function of covariates [16]. In this case, GPP sampling could be optimized and estimated by using (stratified) universal BK instead of (stratified) ordinary BK. Nonhomogeneity in the variance means that the strata exhibit considerable variogram differences [7]. Spatial stratification is a conventional way in surveying stratified heterogeneity [10], [24]. Moreover, heterogeneity in the degree of spatial correlation in different directions can be modelled by a geometric anisotropic variogram model [20]. In summary, it is essential to check the goodness of fit of the models for sampling and estimation. The StrBK model-based approach has only added value when the target variable exhibits meaningful stratified heterogeneity and anisotropy.

The GPP sampling design optimization started with the spatial stratification and variogram calculation. Both of these need prior information about the spatial distribution of the GPP. However, in practice, prior knowledge of GPP is often scarce or unavailable. To solve this problem, we used MODIS GPP as an alternative. This approach assumes that the spatial variability of 1 km spatial resolution MODIS GPP is similar to that of 10 m spatial resolution field measurements of GPP, which is a strong assumption. Although the proxy data may be biased or have a different measurement support, it is considered that they still reasonably represent the spatial covariance structure of the GPP ground data. This assumption should be checked more carefully in future work and alternative proxies such as MODIS NDVI and reflectance, or the spatially distributed output from an ecosystem functional model may also be considered [2]. We also note that the optimized sampling scheme derived in this work is only optimal under the assumptions made by the model used. It is worthwhile to analyse how robust the optimal design is to deviations from the assumptions.

This letter used stratified kriging which assumes zero correlation across stratum boundaries. This assumption may not

be realistic for the real-world situation, and future work might consider relaxing this assumption, by incorporating spatial correlation across stratum boundaries. One such approach might be to include an extra stochastic term that is correlated across stratum boundaries to use the so-called mean of surface with nonhomogeneity method [20], [21].

In addition, the identification of an appropriate strata number may also affect the sampling design of GPP. In principle, the number of strata must be chosen by minimizing the variance of the resulting estimation error. However, in practice, the modeller makes a pragmatic choice by choosing the number of strata such that the main heterogeneities in spatial variation are captured while keeping the number of strata manageable.

With appropriate stratification, StrBK has the advantage that it can generate unbiased estimates for a stratified nonhomogeneity surface when the target variable exhibits considerable differences between strata. A disadvantage may be that, with inappropriate stratification or the assumption of no between-stratum correlation, the sampling design would be no longer optimal. Therefore, it is important to compare the performance of the StrBK model with other models and to strike the right balance between the complexity of a model and its plausibility in real-world situations.

V. CONCLUSION

Spatial sampling is one of the most basic methods to collect information for the estimation of the regional GPP. In this letter, a StrBK model-based sampling approach was proposed to optimize the sampling locations in a spatial heterogeneous area. The method was illustrated with a real-world application in which a sampling strategy was designed for estimation of the regional GPP in the Babao river basin, China. By extending the existing optimization sampling method, the StrBK model-based approach can handle heterogeneities represented by stratification and anisotropy, and can optimize the spatial sampling design for estimation of regional quantities.

ACKNOWLEDGMENT

The authors thank the three anonymous reviewers and the editor for precise and excellent comments that greatly improved this work.

REFERENCES

- [1] S. W. Running, R. R. Nemani, F. A. Heinsch, M. S. Zhao, M. Reeves, and H. Hashimoto, "A continuous satellite-derived measure of global terrestrial primary production," *Bioscience*, vol. 54, no. 6, pp. 547–560, Jun. 2004.
- [2] D. P. Turner, W. D. Ritts, W. B. Cohen, S. T. Gower, S. W. Running, M. S. Zhao, M. H. Costa, A. A. Kirschbaum, J. M. Ham, S. R. Saleska, and D. E. Ahl, "Evaluation of MODIS NPP and GPP products across multiple biomes," *Remote Sens. Environ.*, vol. 102, no. 3/4, pp. 282–292, Jun. 2006.
- [3] A. A. Gitelson, A. Vina, J. G. Masek, S. B. Verma, and A. E. Suyker, "Synoptic monitoring of gross primary productivity of maize using Landsat data," *IEEE Geosci. Remote Sens. Lett.*, vol. 5, no. 2, pp. 133–137, Apr. 2008.
- [4] X. F. Wang, M. G. Ma, G. H. Huang, F. Veroustraete, Z. H. Zhang, Y. Song, and J. L. Tan, "Vegetation primary production estimation at maize and alpine meadow over the Heihe River Basin, China," *Int. J. Appl. Earth Observ. Geoinf.*, vol. 17, pp. 94–101, Jul. 2012.
- [5] M. H. Sales, C. M. Souza, P. C. Kyriakidis, D. A. Roberts, and E. Vidal, "Improving spatial distribution estimation of forest biomass with geostatistics: A case study for Rondonia, Brazil," *Ecol. Modell.*, vol. 205, no. 1/2, pp. 221–230, Jul. 10, 2007.
- [6] S. W. Running, D. D. Baldocchi, D. P. Turner, S. T. Gower, P. S. Bakwin, and K. A. Hibbard, "A global terrestrial monitoring network integrating tower fluxes, flask sampling, ecosystem modeling and EOS satellite data," *Remote Sens. Environ.*, vol. 70, no. 1, pp. 108–127, Oct. 1999.
- [7] J. F. Wang, R. Haining, and Z. Cao, "Sample surveying to estimate the mean of a heterogeneous surface: Reducing the error variance through zoning," *Int. J. Geograph. Inf. Sci.*, vol. 24, no. 4, pp. 523–543, Apr. 2010.
- [8] S. V. Stehman, T. L. Sohl, and T. R. Loveland, "An evaluation of sampling strategies to improve precision of estimates of gross change in land use and land cover," *Int. J. Remote Sens.*, vol. 26, no. 22, pp. 4941–4957, Nov. 20, 2005.
- [9] R. Webster and M. A. Oliver, *Geostatistics for Environmental Scientists*. Chichester, U.K.: Wiley, 2007.
- [10] W. G. Cochran, *Sampling Techniques*, 3rd ed. New York, NY, USA: Wiley, 1977.
- [11] J. J. de Gruijter and C. J. F. ter Braak, "Model-free estimation from spatial samples: A reappraisal of classical sampling theory," *Math. Geol.*, vol. 22, no. 4, pp. 407–415, May 1990.
- [12] D. J. Brus and J. J. de Gruijter, "Random sampling or geostatistical modelling? Choosing between design-based and model-based sampling strategies for soil (with discussion)," *Geoderma*, vol. 80, no. 1/2, pp. 1–44, Oct. 1997.
- [13] R. Vašát, G. B. M. Heuvelink, and L. Borvka, "Sampling design optimization for multivariate soil mapping," *Geoderma*, vol. 155, no. 3/4, pp. 147–153, Mar. 2010.
- [14] J. W. van Groenigen and A. Stein, "Constrained optimization of spatial sampling using continuous simulated annealing," *J. Environ. Qual.*, vol. 27, no. 5, pp. 1078–1086, Sep. 1998.
- [15] A. Stein and C. Ettema, "An overview of spatial sampling procedures and experimental design of spatial studies for ecosystem comparisons," *Agric. Ecosyst. Environ.*, vol. 94, no. 1, pp. 31–47, Jan. 2003.
- [16] D. J. Brus and G. B. M. Heuvelink, "Optimization of sample patterns for universal kriging of environmental variables," *Geoderma*, vol. 138, no. 1/2, pp. 86–95, Feb. 2007.
- [17] J. H. Wang, Y. Ge, G. B. M. Heuvelink, C. H. Zhou, and D. Brus, "Effect of the sampling design of ground control points on the geometric correction of remotely sensed imagery," *Int. J. Appl. Earth Observ. Geoinf.*, vol. 18, pp. 91–100, Aug. 2012.
- [18] J. Ver Hoef, "Sampling and geostatistics for spatial data," *Ecoscience*, vol. 9, no. 2, pp. 152–161, 2002.
- [19] J. de Gruijter, D. J. Brus, M. F. P. Bierkens, and M. Knotters, *Sampling for Natural Resource Monitoring*. Berlin, Germany: Springer-Verlag, 2006.
- [20] M. G. Hu and J. F. Wang, "A spatial sampling optimization package using MSN theory," *Environ. Modell. Softw.*, vol. 26, no. 4, pp. 546–548, Apr. 2011.
- [21] J. F. Wang, G. Christakos, and M. G. Hu, "Modeling spatial means of surfaces with stratified nonhomogeneity," *IEEE Trans. Geosci. Remote Sens.*, vol. 47, no. 12, pp. 4167–4174, Dec. 2009.
- [22] P. Goovaerts, *Geostatistics for Natural Resources Evaluation*. New York, NY, USA: Oxford Univ. Press, 1997.
- [23] A. Huete, C. O. Justice, and W. J. D. van Leeuwen, "MODIS vegetation index (MOD 13)," in *Algorithm Theoretical Basis Document (ATBD) Version 3.0*. Greenbelt, MD, USA: NASA Goddard Space Flight Center, 1999, p. 129.
- [24] L. F. Li, J. F. Wang, Z. D. Cao, and E. Zhong, "An information-fusion method to identify pattern of spatial heterogeneity for improving the accuracy of estimation," *Stochastic Environ. Res. Risk Assessment*, vol. 22, no. 6, pp. 689–704, Oct. 2008.
- [25] P. Diggle and P. J. Ribeiro, *Model-Based Geostatistics*. New York, NY, USA: Springer-Verlag, 2007.
- [26] A. Chorti and D. T. Hristopoulos, "Non-parametric identification of anisotropic (elliptic) correlations in spatially distributed data sets," *IEEE Trans. Signal Process.*, vol. 56, no. 10, pp. 4738–4751, Oct. 2008.